International Journal of Electrical, Electronic and Communication Sciences
ISSN: 2517-9438
Vol:4, No:8, 2010

New Multisensor Data Fusion Method Based on Probabilistic Grids Representation

Zhichao Zhao, Yi Liu, and Shunping Xiao

Abstract—A new data fusion method called joint probability density matrix (JPDM) is proposed, which can associate and fuse measurements from spatially distributed heterogeneous sensors to identify the real target in a surveillance region. Using the probabilistic grids representation, we numerically combine the uncertainty regions of all the measurements in a general framework. The NP-hard multisensor data fusion problem has been converted to a peak picking problem in the grids map. Unlike most of the existing data fusion method, the JPDM method dose not need association processing, and will not lead to combinatorial explosion. Its convergence to the CRLB with a diminishing grid size has been proved. Simulation results are presented to illustrate the effectiveness of the proposed technique.

Keywords—Cramer-Rao lower bound (CRLB), data fusion, probabilistic grids, joint probability density matrix, localization, sensor network.

I. Introduction

THE problem of multisensor data fusion has been of significant interest over the past few years [1]-[7]. Because all sensors have some degree of errors in their measurements, a main challenge is how to combine measurements from different sensors and produce good estimates of the targets. Most of the previous works consider it as an optimization problem with two interrelated functions of association and estimation [4]-[5]. It has been proved that, for more than three sensors, the association of multiple measurements is NP-hard and will lead to combinatorial explosion [4]. If the sensors are passive or there are electronic countermeasures (e.g., range false targets), the association problem is especially difficult [6]-[7]. In this paper, using probabilistic sensor models to handle sensor uncertainty, we propose a new data fusion method called joint probability density matrix (JPDM). The JPDM method has been applied to a multisensor data fusion system. Simulation results show that the accuracy of JPDM approaches to the Cramer-Rao lower bound (CRLB) with a diminishing grid size, and the computational complexity is affordable.

II. Problem Statement

In the multisensor data fusion problem, a set of N targets locate at unknown locations, $\mathbf{x}_j \in \mathrm{R}^2$(generalization to R^3 is easy but not explored here), j = 1, 2, …, N. A centralized sensor network is composed of M sensors distributed at known locations. The sensors can be active or passive, each with a set of detections at the same time with $P_d = 1$ and $P_{fa} \geq 0$.

Z.C. Zhao, Y. Liu, and S.P. Xiao are with the College of Electronic Science and Engineering, National University of Defense Technology, Changsha 410073, China e-mail: zhchzhao@gmail.com

In the presence of additive noise, the measurements can be modeled as follows:

$$\mathbf{z}_{ij} = f_i(\mathbf{x}_j) + \mathbf{v}_{ij}, \quad i = 1, 2, \ldots, M; j = 1, 2, \ldots, N \quad (1)$$

where $\mathbf{z}_{ij}$ denotes noisy measurement of the jth target taking by the ith sensor, f_i is a possibly nonlinear function, and $\mathbf{v}_{ij}$ is an zero-mean i.i.d Gaussian noise with a known covariance matrix $\mathbf{Q}_{ij}$. Thus, the probability density function (PDF) of $\mathbf{z}_{ij}$ is given by

$$p_{ij}(\mathbf{z}_{ij}; \mathbf{x}_j) = \frac{\exp(-\frac{1}{2}(\mathbf{z}_{ij} - f_i(\mathbf{x}_j))^T \mathbf{Q}_{ij}^{-1}(\mathbf{z}_{ij} - f_i(\mathbf{x}_j)))}{2\pi^{m_i/2}|\mathbf{Q}_{ij}|^{1/2}} \quad (2)$$

where m_i is the dimension of $\mathbf{Q}_{ij}$.

The components of the unknown $\mathbf{x}_j$ can be calculated via the maximum likelihood estimate (MLE) technique. The MLE for a vector parameter $\mathbf{x}_j$ is defined to be the value that maximizes the likelihood function $p_j(\mathbf{z}_{1j}, \cdots, \mathbf{z}_{Mj}; \mathbf{x}_j)$ over the allowable values of $\mathbf{x}_j$. Assuming a differentiable likelihood function, the MLE is found by

$$\frac{\partial \ln p_j(\mathbf{z}_{1j}, \cdots, \mathbf{z}_{Mj}; \mathbf{x}_j)}{\partial \mathbf{x}_j} = 0. \quad (3)$$

For our case, because the measurement errors are i.i.d, we have the following expression for the likelihood function:

$$\begin{aligned} L(\mathbf{x}_j) &= p_j(\mathbf{z}_{1j}, \cdots, \mathbf{z}_{Mj}; \mathbf{x}_j) = \prod_{i=1}^{M} p_{ij}(\mathbf{z}_{ij}; \mathbf{x}_j) \\ &= \prod_{i=1}^{M} \frac{\exp(-\frac{1}{2}(\mathbf{z}_{ij} - f_i(\mathbf{x}_j))^T \mathbf{Q}_{ij}^{-1}(\mathbf{z}_{ij} - f_i(\mathbf{x}_j)))}{2\pi^{m_i/2}|\mathbf{Q}_{ij}|^{1/2}}. \end{aligned} \quad (4)$$

The maximization problem to solve is

$$\hat{\mathbf{x}}_j = \arg\max_{\mathbf{x}_j} L(\mathbf{x}_j) = \arg\max_{\mathbf{x}_j} \ln L(\mathbf{x}_j). \quad (5)$$

Our goal is to estimate all unknown parameters $\mathbf{x}_j$ in a feasible way, which will not lead to combinatorial explosion.

III. The JPDM Method

A general data fusion framework is proposed in this section. Using this framework, various kinds of measurements from different sensors can be combined together.

A. Probabilistic Sensor Models

Each sensor has a probabilistic model, which interprets its measurements using some PDF over the range of possible values. Here, we state three kinds of measurements that are often used in multisensor system. To reduce the computational complexity, we restrict the calculation in a $k - \sigma$ region. The value of k is always set to 3, which gives a 99.7% probability that the target falls within the gate.

1) Angle of Arrival Measurements: Sometimes, only the angle of arrival (AOA) is available. Suppose the measurement error in the AOA is Gaussian. Thus, given a measurement, θ_i, we can write the PDF of the target being located at some point (x, y), as follows:

$$p(x,y|\theta_i) = \begin{cases} \frac{1}{\sqrt{2\pi}\sigma_{\theta i}} \exp(-\frac{(\theta-\theta_i)^2}{2\sigma_{\theta i}^2}), & |\theta-\theta_i| \le k\sigma_{\theta i} \\ 0, & otherwise \end{cases} \tag{6}$$

where $\sigma_{\theta i}$ is the standard deviation of AOA measurement error for sensor i, $\theta = \arctan((y-y_i)/(x-x_i))$, ($x_i$, y_i) is the location of sensor i.

Because no range information is available, we assume the range uniformly distributed between $r_{\min}$ and $r_{\max}$. Thus,

$$\begin{aligned} &p(x,y|r_i,\theta_i) = p(x,y|r_i)p(x,y|\theta_i) \\ &= \begin{cases} \frac{\exp(-\frac{(\theta-\theta_i)^2}{2\sigma_{\theta i}^2})}{\sqrt{2\pi}\sigma_{\theta i}(r_{\max}-r_{\min})}, & |\theta-\theta_i| \le k\sigma_{\theta i}, r_{\min} \le r_i \le r_{\max} \\ 0, & otherwise \end{cases} \end{aligned} \tag{7}$$

2) Time of Arrival Measurements: Sometimes, only the time of arrival (TOA) is available. Suppose the measurement error in the TOA is Gaussian. Thus, given a measurement, τ_i, we can write the PDF of the target being located at some point (x, y), as follows:

$$p(x,y|c\tau_i) = \begin{cases} \frac{1}{\sqrt{2\pi}c\sigma_{\tau i}} \exp(-\frac{(r-c\tau_i)^2}{2c^2\sigma_{\tau i}^2}), & |r-c\tau_i| \le kc\sigma_{\tau i} \\ 0, & otherwise \end{cases} \tag{8}$$

where $\sigma_{\tau i}$ defines the standard deviation of the TOA measurement error for sensor i, $r = \sqrt{(x-x_i)^2+(y-y_i)^2}$, c is the velocity of light.

Because no azimuth information is available, we assume the azimuth uniformly distributed between $\theta_{\min}$ and $\theta_{\max}$. Thus,

$$\begin{aligned} &p(x,y|c\tau_i,\theta_i) = p(x,y|c\tau_i)p(x,y|\theta_i) \\ &= \begin{cases} \frac{\exp(-\frac{(r-c\tau_i)^2}{2c^2\sigma_{\tau i}^2})}{\sqrt{2\pi}c\sigma_{\tau i}(\theta_{\max}-\theta_{\min})}, & |r-c\tau_i| \le kc\sigma_{\tau i}, \\ & \theta_{\min} \le \theta_i \le \theta_{\max} \\ 0, & otherwise \end{cases} \end{aligned} \tag{9}$$

3) TOA and AOA Measurements: Sometimes, both the TOA and AOA are available. Given the measurement, τ_i and θ_i, we can write the PDF of the target being located at some point (x, y), as follows:

$$\begin{aligned} &p(x,y|c\tau_i,\theta_i) = p(x,y|c\tau_i)p(x,y|\theta_i) \\ &= \begin{cases} \frac{\exp(-\frac{\sigma_{\theta i}^2(r-c\tau_i)^2+c^2\sigma_{\tau i}^2(\theta-\theta_i)^2}{2c^2\sigma_{\tau i}^2\sigma_{\theta i}^2})}{2\pi c\sigma_{\tau i}\sigma_{\theta i}}, & |r-c\tau_i| \le kc\sigma_{\tau i}, \\ & |\theta-\theta_i| \le k\sigma_{\theta i} \\ 0, & otherwise \end{cases} \end{aligned} . \tag{10}$$

B. Probabilistic Grids Representation

Conversion of all sensor observations to a common format is a basic requirement for all multisensor data fusion systems [2]. Since sensor measurements are often acquired in local polar coordinates, a transform to Cartesian coordinates must be included. But the transformation is nonlinear, the joint PDF in (4) is hard to calculate. So we use a probabilistic grids representation, which comes from the concept of occupancy grid [8]. Occupancy grid was first introduced by Moravec and Elfes for robotic mapping [9], and has been widely used for environment modeling in robotics due to the simplicity of its implementation [10].

Suppose an area of interest (AOI) have a length, L, and a width, W. Choosing a sampling interval, d, the AOI can be divided into a grid of equal sized spatial cells. Each cell is indexed and labeled with a property, thus the state s_{lw} may describe a two dimensional world indexed by *lw* and having the property s. We store all the states in a $K_L \times K_W$ matrix, where $K_L = L/d, K_W = W/d$. Thus, the joint PDF in (4) can be calculated cell by cell in a discrete sampled form.

C. PDM and joint PDM

In our case, interest is focused on the probability distribution of possible target in each grid cell. So, given a measurement, Θ, we let s_{lw} denote the probability that Θ comes from a target located in cell *lw*:

$$s_{lw} = \frac{1}{C}p((l,w)|\Theta) \tag{11}$$

where C is a normalizing constant obtained by summing all the conditional probabilities to one, that is

$$C = \sum_{l=1}^{K_L}\sum_{w=1}^{K_W} p((l,w)|\Theta). \tag{12}$$

For each measurement of each sensor, using (7), (9) or (10), we can calculate all s_{lw} cell by cell, and store them in a $K_L \times K_W$ matrix. Thus, for the jth measurement of the ith sensor, there is a corresponding matrix, $\mathbf{P}_{ij}$. Summing all $\mathbf{P}_{ij}$ of the ith sensor together, we get

$$\mathbf{P}_i = \sum_{j=1}^{N_i} \mathbf{P}_{ij} \tag{13}$$

where, N_i is the number of measurements observed by the$i$th sensor, which may be larger or equal to N. Because $\mathbf{P}_i$ describes the probability distribution of all measurements acquired by the ith sensor, we call $\mathbf{P}_i$ the probability density matrix (PDM) of sensor i.

Calculating PDMs of all the sensors and combining them together, we get a joint PDM, $\mathbf{P}$. Computationally, $\mathbf{P}$ is a simple point-wise multiplication of every $\mathbf{P}_i$, i.e., the *lw* element of $\mathbf{P}$ is

$$\mathbf{P}(l,w) = \prod_{i=1}^{M} \mathbf{P}_i(l,w) = \prod_{i=1}^{M}\sum_{j=1}^{N_i} \mathbf{p}_{ij}(l,w) \tag{14}$$

D. Peaks in the joint PDM

Peaks in the joint PDM imply that targets are more likely to be located there, so we can take these peaks as the estimated position of targets. Consequently, the number of peaks can be considered as the number of targets. Mapping values of the joint PDM to a gray map (deep color region corresponds to large value of the density), the multisensor data fusion problem can be converted to a peak picking problem in the grids map.

IV. Simulation Results

Simulations have been conducted to demonstrate the performance of the proposed method, as shown in Fig. 1. In Cartesian coordinates, three sensors with $\sigma_r = 10m$ and $\sigma_\theta = 1^\circ$ are sited at (0, 0), (1000, 0) and (500, 866), respectively. Four targets are randomly generated near the

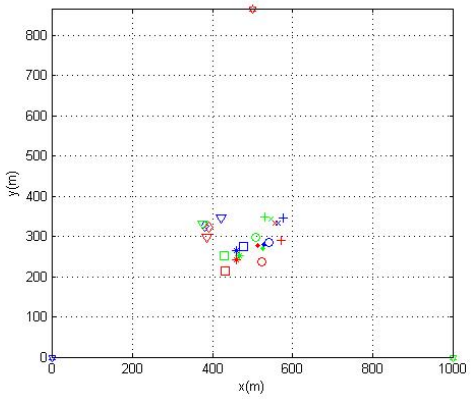

Fig. 1. Sensors and measurements in the simulation scenario.

center of the common work space, each accompanied by a range false target about $5m$ away from the true one in the corresponding sensor. Therefore, each sensor can detect eight targets at the same time.

Using (13), we can calculate PDMs of all sensors, then simply add them together, we get the uncertainty region of all measurements, as shown in Fig. 2. From Fig. 1 and Fig. 2, we can see that it is difficult to distinguish which three measurements are from the same target. Fig. 3 illustrates the

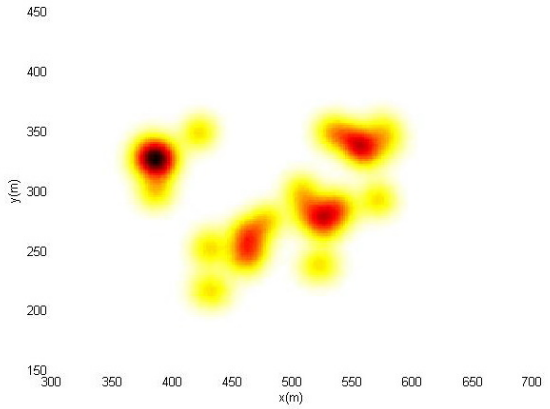

Fig. 2. Uncertainty regions of all measurements.

joint PDM computed by (14). Four peaks can be seen clearly, which denote the estimated position of four targets. All the false targets have been eliminated successfully. Mapping Fig. 3 to a 2D map, we get Fig. 4. Compared with Fig. 2, the area of uncertainty region in Fig. 4 has reduced remarkably, which means that the accuracy has been improved. Four deep colored

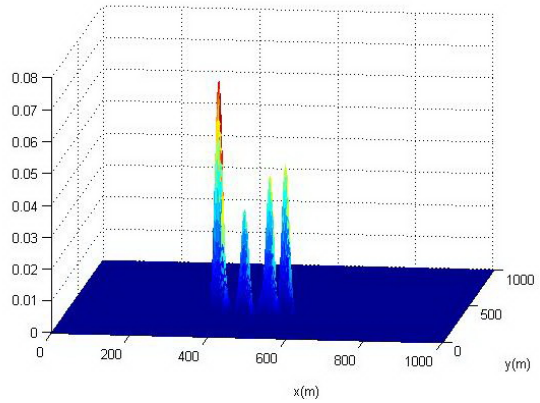

Fig. 3. Joint PDM: four peaks corresponding to the position of four targets.

region imply that there are four real targets. The darkest point in each region represents the estimated position of the corresponding target. The estimated position and true position

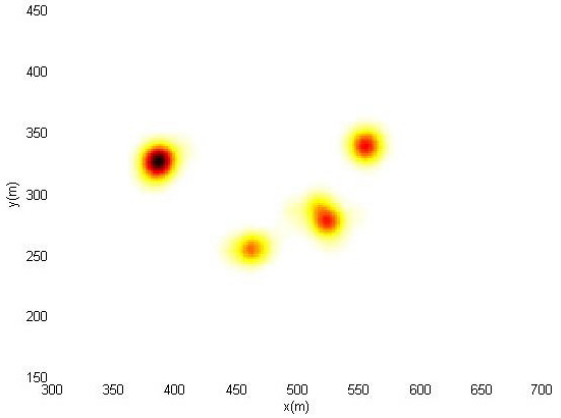

Fig. 4. The 2D gray map of Fig. 3.

of the four targets are shown in Table I. From where we can see that the position error is small and acceptable. The Cramer-Rao

TABLE I
Position Error of JPDM

Position(m)	Target 1	Target 2	Target 3	Target 4
True	(388.6,322.4)	(450.6,254.2)	(514.1,273.7)	(558.1,320.9)
Estimated	(386,324)	(460,254)	(522,278)	(554,330)
Error	3.05	9.40	8.99	9.98

inequality sets a lower bound for the variance of any unbiased parameter estimations. Hence it is of interest to compare the performance of the JPDM method with the optimum. We use the same scenario, except that only one target is observed. In this case, the root mean square (RMS) error was averaged over 1000 independent Monte-Carlo runs. To study the influence introduced by the size of grid cell, two kinds of grids are used. As shown in Table II, there is good agreement between the simulation results and the analytical evaluation of the CRLB. For $5m \times 5m$ grid, the RMS error is 2.8% higher than the

TABLE II
AVERAGE RMS POSITION ERROR OF 1000 MONTE-CARLO

	JPDM *(5mX5m)*	JPDM *(1mX1m)*	CRLB
RMS error (m)	8.4283	8.3052	8.1960
Elapsed Time (ms)	7.80	237.2	-

CRLB, for $1m \times 1m$ grid, it is only 1.3% higher than the CRLB. From Table II, comparing the RMS error and elapsed time of $1m \times 1m$ grid with that of $5m \times 5m$ grid, we can see that: while the size of grid decreases to 20%, the computational cost increases to 3000%, approximately with square of the number of grid cells, however, the RMS error only decreases to 98.5%. So, there is a trade-off of accuracy and computational complexity. In practice, taking d as 1/2 $\sim$ 1/5 of the desired accuracy is sufficient.

V. CONCLUSION

A new multisensor multitarget data fusion method has been presented. Since the JPDM method does not require sensor measurement errors to be normally distributed, it is useful for a variety of applications. Simulation results have shown that this novel approach provides average RMS errors that are close to the CRLB. This method does not need additional association processing, and will not lead to combinatorial explosion. The cost of computational complexity is of $O(M \times N \times K_L \times K_W)$for $M-$sensor N-target over a $K_L \times K_W$grid. Like the Hough Transform, multi-resolution technology can be used to decrease the computational complexity further. Also, other information, such as frequency and RCS, can be integrated in this method. Future research includes apply it to emitter localization and target recognition in complex electromagnetic environment where $P_d \leq 1$ and $P_{fa} \geq 0$.

REFERENCES

[1] M. E. Liggins, D. L. Hall, J. Llinas, Handbook of Multisensor Data Fusion: Theory and Practice. Boca Raton, FL: CRC Press, 2009.
[2] H. B. Mitchell, Multi-Sensor Data Fusion. Berlin: Springer, 2007.
[3] X. Sheng, Y. Hu, "Maximum likelihood multiple-source location using acoustic energy measurements with wireless sensor network," IEEE Trans. Signal Process., vol. 53, no 1, pp. 44-53, Jan. 2005.
[4] D. Somnath, Y. Murali, P. Krishna, and Y. Bar-Shalom, "A generalized S-D assignment algorithm for multisensor-multitarget state estimation," IEEE Trans. Aerosp. Electron. Syst., vol. 33, no. 2, pp. 523-538, Apr. 1997.
[5] T. Kirubarajan, H. Wang, Y. Bar-Shalom, and K. R. Pattipati, "m-Best S-D assignment algorithm with application to multitarget tracking," IEEE Trans. Aerosp. Electron. Syst., vol. 37, no. 1, pp. 22-39, Jan. 2001.
[6] S. Deb, K. R. Pattipati, and Y. Bar-Shalom, "A multisensor-multitarget data association algorithm for heterogeneous sensors," IEEE Trans. Aerosp. Electron. Syst., vol. 29, no. 2, pp. 560-568, Apr. 1993.
[7] D. Musicki, "Multi-Target Tracking using Multiple Passive Bearings-Only Asynchronous Sensors," IEEE Trans. Aerosp. Electron. Syst., vol. 44, no. 3, pp. 1151-1160, July 2008.
[8] A. Elfes, "Sonar-based real-world mapping and navigation," IEEE Trans. Robot. Autom., vol. 3, no. 3, pp. 249-265, June 1987.
[9] H. P. Moravec, and A. Elfes, "High resolution maps from wide angle sonar," in Proc. IEEE Conf. Robotics and Automation, pp. 116-121, 1985.
[10] A. Birk, S. Carpin, "Merging occupancy grid maps from multiple robots," Proc. IEEE, vol. 94, no. 7, pp. 1384-1397, July 2006.

Zhichao Zhao He is a Ph. D. candidate in National University of Defense Technology (NUDT). His research mainly focuses on multi-sensor information fusion, radar data processing and radar electronic warfare.